UCSF

UC San Francisco Previously Published Works

Title

A novel mouse model of hindlimb joint contracture with 3D-printed casts

Permalink

https://escholarship.org/uc/item/3020r7vs

Journal

Journal of Orthopaedic Research®, 40(12)

ISSN

0736-0266

Authors

Moore, Laura K

Lee, Carlin S

Agha, Obiajulu

et al.

Publication Date

2022-12-01

DOI

10.1002/jor.25313

Peer reviewed

A novel mouse model of hindlimb joint contracture with 3D-printed casts

Laura K. Moore[1], **Carlin S. Lee**[2], **Obiajulu Agha**[1], **Mengyao Liu**[1,2], **He Zhang**[1,2,3], **Alan B. C. Dang**[1,2], **Alexis Dang**[1,2], **Xuhui Liu**[2], **Brian T. Feeley**[1,2]

[1]Department of Orthopedic Surgery, University of California San Francisco, San Francisco, California, USA

[2]Department of Orthopedic Surgery, San Francisco VA Medical Center, San Francisco, California, USA

[3]Department of Exercise Physiology, Beijing Sport University, Beijing, China

Abstract

Stiff joints formed after trauma, surgery or immobilization are frustrating for surgeons, therapists and patients alike. Unfortunately, the study of contracture is limited by available animal model systems, which focus on the utilization of larger mammals and joint trauma. Here we describe a novel mouse-based model system for the generation of joint contracture using 3D-printed clamshell casts. With this model system we are able to generate both reversible and irreversible contractures of the knee and ankle. Four- or 8-month-old female mice were casted for either 2 or 3 weeks before liberation. All groups formed measurable contractures of the knee and ankle. Younger mice immobilized for less time formed reversible contractures of the knee and ankle. We were able to generate irreversible contracture with either longer immobilization time or the utilization of older mice. The contracture formation translated into differences in gait, which were detectable using the DigiGait® analysis system. This novel model system provides a higher throughput, lower cost and more powerful tool in studying the molecular and cellular mechanisms considering the large existing pool of transgenic/knockout murine strains.

Keywords

arthrofibrosis; contracture; gait analysis; mouse; stiff joint

1 | INTRODUCTION

Stiff joints, also known as joint contractures, present a frustrating treatment challenge for surgeons, therapists, and patients alike. Limitations in joint motion lead to difficulty performing activities of daily living, increased energy expenditure, and pain.[1,2] Unfortunately, contracture formation is exceedingly common after injury or immobilization.[3,4] Loss of the terminal 5–15° of extension after elbow dislocation is expected.[5,6] One percent of anterior cruciate ligament injuries managed nonoperatively eventually require surgical contracture release,[7] and up to 57% after a knee dislocation event.[8] Current treatment options include intensive physical or occupational therapy, serial casting, dynamic splinting, and surgical release.[8,9]

Anecdotal evidence suggests that age plays a key role in the development of contractures, with pediatric patients being more likely to recovery joint mobility over time. However, the actual relationship between age and contracture formation appears to be more complex. Increasing age appears to be a modest risk factor for the formation of severe contracture after elbow trauma.[10] However, younger patients have less reliable response to elbow contracture release[11] and are at higher risk for arthrofibrosis after Anterior cruciate ligament reconstruction.[12]

The study of contracture formation and prevention is limited by the availability of model systems. Current animal models utilize rats, rabbits or dogs.[13–16] Although these model systems provide useful information, they have a number of limitations. First, with the exception of the canine model, which is based on application of a shoulder spica cast, all of these animal models are reliant on a surgical intervention. This can cloud the picture when it comes to contracture formation, as it does not differentiate immobilization-based contracture from posttraumatic and postsurgical. Although there may be significant overlap in terms of pathophysiology, these models do not allow for their study. Second, the reliance on larger mammals slows research by increasing costs and decreasing throughput. It also limits the utilization of the wide array of mouse models of disease and transgenic systems that are already available.

For this reason, we have sought to generate a novel mouse model of immobilization-based joint contracture. Because of advances in three-dimensional (3D) printing technology, we are now able to develop and produce complex shapes with much higher speed and throughput than previous technologies allowed. Here we are able to generate 3D printed casts or fracture braces for mouse limb immobilization. This technique closely recapitulates the human phenotype, where prolonged immobilization in a cast or fracture brace causes contracture formation.

2 | MATERIAL AND METHODS

2.1 | 3D-Printing of clamshell casts

Based on mouse measurements 3D-printed clamshell-type casts were designed in AutoDesk Fusion 360 (Figure 1A). The cast design was modified in an iterative fashion to provide a best fit for the mouse hindlimb with the knee in 90° of flexion and ankle in 130° of

dorsiflexion. Preliminary casts were printed on in polylactic acid using a Prusa MK3 3D printer. Final casts were printed on a FormLabs Form2 3Dprinter using their proprietary methacrylate-based resin (Figure 1B, STL files available in Supporting Information Materials). The top of the cast was lined with 0.04″ adhesive felt to minimize skin irritation.

2.2 | Mouse hindlimb immobilization

Four- or 8-month-old female C57BL/J6 had a single hind limb immobilized using the custom cast for a total of 2 ($n = 4$ mice) or 3 weeks ($n = 3$ mice). Mice were anesthetized using isoflurane anesthesia (1%–4% inhaled) for cast placement and motion assessment. Casts were secured using 20G wire placed through pretemplated grooves on the cast (Figure 1C). Casts were then removed after either 14 or 21 days. Motion was assessed before casting and at 0, 4, 7, 14, and 21 days after cast removal. Range of motion (ROM) was assessed using a goniometer and compared to the contralateral limb, which was used as an internal control. Mice were cared for in accordance with the guidelines set by the National Institutes of Health (NIH) on the care and use of laboratory animals. All mouse experiments were completed with the approval of the Veterans Administration Institutional Animal Care and Use Committee (Protocol #17-020). The studies were powered to detect a difference of 25° assuming a standard deviation of 10°, which was based on preliminary data.

2.3 | ROM assessment

ROM was assessed on each mouse before casting and at 0, 4, 7, 14, and 21 days after cast removal. Measurements were taken on the treated and untreated knee and ankle at each time point. Motion was assessed using a goniometer. The tibia or femur were held in line with one arm of the goniometer with a set of forceps while the distal limb was moved with a second set of forceps. The joint was taken through an arc of motion up to the point that any resistance was met. Terminal flexion and extension were recorded. Measurement system reproducibility was confirmed during pilot studies. To maintain consistency, all measurements were completed by one of two researchers who were trained in the methodology and had previously confirmed their reproducibility (Dr. Moore and Dr. Agha).

2.4 | DigiGait®

To assess for any changes in gait pattern due to hindlimb contracture in depth gait analysis was also completed for each mouse using DigiGait® system (Mouse Specifics, Inc.). DigiGait® was completed before immobilization and on Days 0, 4, 7, 14, and 21. Mouse gait was assessed at a belt speed of 10 cm/s and neutral inclination.

2.5 | Histopathology

Eight-month-old mice ($n = 3$) were killed upon study completion in accordance with IACUC protocols. Both hindlimbs were excised and extra soft tissues were removed before fixation in 4% paraformaldehyde overnight at 4°C. Tissues were then decalcified for a minimum of 1 week in 10 mM ethylenediaminetetraacetic acid. Tissues were then embedded in paraffin. Sections were then stained with hematoxylin and eosin (H&E) or picrosirius red according to laboratory protocols.

2.6 | Data analysis

Data were analyzed in Microsoft Excel and GraphPad Prism. All statistics were completed in GraphPad Prism. ROM and gait characteristics were compared using two-way analysis of variance (ANOVA) or mixed-effects model with a significance level of 0.05 and a Bonferroni correction for multiple comparisons where appropriate. For ROM analysis standard deviation includes the assumed measurement error of 5°, as measurements could not be made more accurately than this.

3 | RESULTS

3.1 | Immobilization and motion measurement

We found that immobilization of a mouse single hind limb of resulted in measurable joint contractures of both the knee and the ankle (right leg). The casts were well tolerated by the mice and did not slip off or break. More than 30 mice were immobilized over the pilot and publication studies and only one mouse experienced cast loss, which was later determined to be a technical error related to wire placement. The cast design is readily modifiable and can be easily adjusted to fit mice of differing weights, strains, or genders. The contractures were readily detectable using both a goniometer and the DigiGait® system. Reproducibility of the goniometer-based measurement system was assessed by comparing baseline measurements across the three presented studies (Table S1). Measurements were found to be reproducible across studies and across trained researchers, with a pooled standard deviation of 10.03 for the knee and 5.33 for the ankle. There were no significant differences in the measurements between measurements on the right and left limbs.

3.2 | Week Immobilization

Immobilization of 4-month-old mice for 2 weeks resulted in reversible contracture formation of the knee and ankle. Peak motion loss for the knee was observed on Day 0 after release from immobilization for the knee and Day 4 for the ankle (Table 1). For the knee, the average arc of motion was $91.3 \pm 18°$ for the right (immobilized) knee compared to $128.7 \pm 8.6°$ for the left (control) knee, resulting in an average motion loss of $37 \pm 10.4°$ of knee motion (Figure 2A and Table 1). For the ankle, the average arc of motion was $55.0 \pm 7.1°$ for the right (immobilized) ankle compared to 142.5 ± 2.9 for the left (control) ankle, resulting in an average motion loss of $80.0 \pm 14.6°$ (Figure 2B and Table 1). After cast removal, knee and ankle motion gradually returned to baseline over the course of 14 days. These changes were also detectable using the DigiGait® gait analysis system using multiple output metrics including Stance Swing % (Figures 2C and S1).

3.3 | Three-week immobilization

Similar to mice immobilized for 2 weeks, mice immobilized for 3 weeks demonstrated peak motion loss on Day 0 for the knee and Day 3 for the ankle (Table 1). For the knee, total motion on Day 0 for the immobilized (right) knee was 93.3 ± 11.6 and $133.3 \pm 2.9°$ for the control (left) limb, resulting in an average loss of knee motion of $40.0 \pm 8.4°$ (Figure 3A and Table 1). For the ankle on Day 3, total motion was $73.3 \pm 2.9°$ for the immobilized (right) ankle and 166.7 ± 2.9 for the control (left) ankle, resulting in an average loss of 93.6

± 2.89° of ankle motion (Figure 3B and Table 1). In contrast to the 2-week immobilization group, the 3-week group did not demonstrate complete recovery of knee or ankle ROM after cast liberation. Three weeks after liberation from the cast the mice demonstrated persistent loss of 26.7 ± 4.1° at the ankle and 63.3 ± 4.56° at the ankle. These differences in motion were also detectable using multiple DigiGait® parameters, including propel stride percentage (Figures 3C and S2). Although the mice lost both knee flexion and extension, the persistent motion loss came in the form of a knee flexion contracture (Table 1). Similarly, the persistent motion loss at the ankle was predominantly due to a dorsiflexion contracture (Table 1).

3.4 | Old mouse immobilization

In contrast to the younger (4-month-old mice) immobilized for 2 weeks, older mice (8-month-old) responded more quickly to immobilization. When immobilized for 2 weeks the older mice demonstrated peak motion loss in the knee on Day 3 and the ankle on Day 0. On Day 0, we observed a total arc of motion of 73.5 ± 11.1 for the immobilized (right) ankle and 162.5 ± 2.9 for the control (left) ankle, resulting in a peak motion loss of 88.75 ± 8.1° (Figure 4A and Table 1). However, after 21 days of liberation, ankle motion returned to near normal with a persistent loss of 28.4 ± 8.9° (Figure 4A and Table 1). The difference in motion between old and young mice was significantly significant on Day 3 (p = 0.04, young>old) and Day 14 (p = 0.028, old>young). Given the reversal in direction of significance and marginal p values we feel this is unlikely to represent a real effect.

Similar to the younger mice, the total arc of motion was 77.0 ± 16.5 for the immobilized (right) knee and 143.0 ± 4.5 for the control (left) knee, resulting a peak loss of knee motion of 66.0 ± 12° (Figure 4B and Table 1). However, in contrast to the younger mice immobilized for 2 weeks, the older mice did not demonstrate complete recovery of motion (Figure 4B, ANOVA, $p < 0.0001$ for age). Upon study completion the older mice were left with a persistent loss of 40 ± 9.12° in the immobilized (right) knee compared to the control (left) knee.

3.5 | Histopathology

Histopathologic evaluation was completed on the 8-month-old mice that were immobilized for 2 weeks upon study completion. Due to their small size ankle sections were subjected to H&E staining only (Figure 5). Sections of the immobilized limbs demonstrated synovial thickening and increased extracellular matrix (ECM) deposition in both the anterior and posterior ankle when compared to previously published studies.[17] Knee sections were subjected to H&E (Figure 6) as well as picrosirius red staining (Figure S3). H&E staining demonstrated synovial thickening and increased ECM deposition in the immobilized knees, which was more pronounced in the posterior knee. This was accompanied by a loss of synovial folding, which is consistent with the knee flexion contractures observed in this group (Table 1). Picrosirius red staining confirmed a modest increase in collagen deposition in both the anterior fat pad and posterior knee (Figure S3).

4 | DISCUSSION

In this study we assess the degree and duration of contracture formation after immobilization of a single mouse hindlimb with a 3D-printed clamshell cast. The clamshell casts can be readily modified to fit other genders, strains and weights of mouse and potentially larger mammals. The casts are also economical, with production cost of $1.26 each. The changes in joint function are detectable both by measuring ROM and by rodent gait analysis. Both the STL and computer aided design files are available in the supplementary information so they can be utilized by other research groups.

We have found that longer duration of immobilization (2 vs. 3 weeks, Figures 2 and 3) results in the formation of irreversible contracture formation for both the knee and the ankle. This is consistent with human literature on both posttraumatic and immobilization based contracture formation, where longer duration of immobilization is associated with more severe and contracture formation.[4–6,18,19] At this time it is unclear if the transition between sustained and reversible contracture formation is due to the magnitude of periarticular fibrosis or activation of differing molecular pathways. Elucidation of the mechanisms of sustained as compared to reversible contracture formation has the potential to profoundly impact clinical practice and is the subject of ongoing investigations.

Although the DigiGait® system is a powerful tool for detecting changes in gait, we found that only a few parameters reached statistical significance for this study (Figures 3C, 4C, S1, and S2). This is likely due in part to the small sample size presented in this study. Parameters that did reach statistical significance for this study were largely related to the stance time or stride length. In general, the mice appeared to spend less time in stance on the immobilized leg, suggesting that the limb was either painful or that they needed more time to accommodate the stiff limb (Figures 2C, 3C, and S2). Furthermore, we see that stride time and stride length have statistically significant changes over time, but not between sides (Figure S1). Although there were not statistically significant differences between sides, this data indicates that immobilization and contracture have a measurable impact on overall gait.

The hypothesis that the limb may be painful after release from immobilization is consistent with the ROM data showing that knee and ankle motion often worsen immediately after release from immobilization, before improving (Figures 2B, 3B, and 4A,B). It is likely that the animals may experience some pain and inflammation after release from immobilization due to breakup of periarticular adhesions. Additionally, previous studies have also reported the presence of hyperalgesia in rats after cast removal,[20] suggesting that overall sensitization of the limb may play a role.

In addition to duration of immobilization, we see that animal age impacts motion recovery. We see that when older mice are immobilized, they form contracture more rapidly requiring only 2 weeks of immobilization to produce a similar magnitude of contracture formation as younger mice immobilized for 3 weeks. Interestingly, the older mice generally recovered their ankle motion, however, were left with persistent knee flexion contractures (Figure 4B). In contrast to duration of immobilization, the impact of age on contracture formation appears to be a more complicated question in human studies. With increasing age we see

reduced muscle elasticity combined with increased tendon stiffness and loss of tendon strength,[21] which may lead to either increased or decreased stiffness depending on the situation. Further clouding the picture is the fact that elderly and youthful patients tend to suffer very different injury patterns. That said, age was not found an independent risk factor for the development of immobilization-based contractures[22] or contracture formation after elbow dislocation.[10] In contrast, young patients appear to undergo procedures to manage stiffness more frequently than elderly patients.[12,23] However, it may be that we are simply less tolerant of limitations in motion in younger patients as opposed to the elderly, as opposed to any increase severity of contracture formation. Perhaps using this model, we will be able to elucidate some of the pathophysiological issues that arise with aging tissues and immobilization.

The preliminary histopathology presented in this study indicates that immobilization-based contracture may be driven by fibrosis of periarticular tissues. Our findings in the knee are consistent with previous reports on rodent immobilization, where knee flexion contracture is associated with loss of synovial thickening, excess ECM deposition, and posterior capsule shortening.[24–26] The histopathologic changes were also evident in the ankle, where we observed increased ECM deposition in the anterior and posterior ankle. Interestingly, these changes are present despite near complete ankle motion recovery in the older mouse group. This suggests that there may be persistent changes in the periarticular soft tissues that merit further investigation. Work on elucidating the underlying differences between transient and persistent joint contracture is ongoing.

The model presented in this study presents a number of advantages over previously published models. First, as discussed above, it closely recapitulates the human phenotype. Second, by utilizing the mouse as a model organism, as opposed to larger mammals, this model provides a more powerful tool in studying the molecular and cellular mechanisms considering the existing large pool of transgenic/knockout murine strains. It will also reduce study costs and boost throughput compared to larger mammal studies. Third, the model does not require any trauma to the joint. This simplifies both protocol implementation and the interpretation of results. This model system is readily modifiable and could be easily adapted to study numerous related pathologies including posttraumatic joint contracture, hindlimb fracture, tendon and ligament injuries. And finally, to our knowledge this is the first report of a 3D-printed cast or fracture brace designed for the mouse.

5 | CONCLUSIONS

The work here presents a novel, clinically relevant and humane method for the generation of both reversible and irreversible hindlimb contractures in the mouse. This model closely recapitulates the human phenotype where longer immobilization produces sustained contracture formation (Figure 3). Additionally, we find that older mice develop sustained contractures with shorter immobilization time (Figure 4). This model system is readily modifiable and will allow for more in-depth study of contracture formation through the large pool of already available transgenic mice. This system has the potential to dramatically reduce cost and increase throughput, thereby enhancing our ability to study the multitude of risk factors for and ramifications of contracture formation.

Supplementary Material

Refer to Web version on PubMed Central for supplementary material.

REFERENCES

1. Waters RL, Mulroy S. The energy expenditure of normal and pathologic gait. Gait Posture. 1999;9(3):207–231. [PubMed: 10575082]

2. Prilutsky BI, Petrova LN, Raitsin LM. Comparison of mechanical energy expenditure of joint moments and muscle forces during human locomotion. J Biomech. 1996;29(4):405–415. [PubMed: 8964770]

3. Lindenhovius ALC, Jupiter JB. The posttraumatic stiff elbow: a review of the literature. J Hand Surg Am. 2007;32(10):1605–1623. [PubMed: 18070653]

4. Haller JM, Holt DC, McFadden ML, Higgins TF, Kubiak EN. Arthrofibrosis of the knee following a fracture of the tibial plateau. Bone Jt J. 2015;97-B(1):109–114.

5. Schippinger G, Seibert FJ, Steinböck J, Kucharczyk M. Management of simple elbow dislocations: does the period of immobilization affect the eventual results? Langenbeck's Arch Surg. 1999;384(3): 294–297. [PubMed: 10437619]

6. Iordens GIT, Van Lieshout EMM, Schep NWL, et al. Early mobilisation versus plaster immobilisation of simple elbow dislocations: results of the FuncSiE multicentre randomised clinical trial. Br J Sports Med. 2017;51(6):531–538. [PubMed: 26175020]

7. Sanders TL, Kremers HM, Bryan AJ, Kremers WK, Stuart MJ, Krych AJ. Procedural intervention for arthrofibrosis after ACL reconstruction: trends over two decades. Knee Surg Sport Traumatol Arthrosc. 2017;25(2):532–537.

8. Magit D, Wolff A, Sutton K, Medvecky MJ. Arthrofibrosis of the knee. J Am Acad Orthop Surg. 2007;15(11):682–694. [PubMed: 17989419]

9. Nandi S, Maschke S, Evans PJ, Lawton JN. The stiff elbow. Hand. 2009;4(4):368–379. [PubMed: 19350328]

10. Qian Y, Yu S, Shi Y, Huang H, Fan C. Risk factors for the occurrence and progression of posttraumatic elbow stiffness: a case-control study of 688 cases. Front Med. 2020;7:604056.

11. Stans AA, Maritz NGJ, O'Driscoll SW, Morrey BF. Operative treatment of elbow contracture in patients twenty-one years of age or younger. J Bone Jt Surg Ser. 2002;84(3):382–387.

12. Huleatt J, Gottschalk M, Fraser K, et al. Risk factors for manipulation under anesthesia and/or lysis of adhesions after anterior cruciate ligament reconstruction. Orthop J Sport Med. 2018;6(9):232596 90.

13. Chahla J, Dean CS, Moatshe G, et al. Meniscal ramp lesions: anatomy, incidence, diagnosis, and treatment. Orthop J Sport Med. 2016;4(7):313–320.

14. Dunham CL, Castile RM, Havlioglu N, Chamberlain AM, Galatz LM, Lake SP. Persistent motion loss after free joint mobilization in a rat model of posttraumatic elbow contracture. J Shoulder Elb Surg. 2017;26(4):611–618.

15. Lake SP, Castile RM, Borinsky S, Dunham CL, Havlioglu N, Galatz LM. Development and use of an animal model to study posttraumatic stiffness and contracture of the elbow. J Orthop Res. 2016;34(2): 354–364. [PubMed: 26177969]

16. Schollmeier G, Sarkar K, Fukuhara K, Uhthoff HK. Structural and functional changes in the canine shoulder after cessation of immobilization. Clin Orthop Relat Res. 1996;323:310–315.

17. Kim AR, Kim HS, Kim DK, et al. The extract of Chrysanthemum zawadskii var. latilobum ameliorates collagen-induced arthritis in mice. Evid Based Complement Alternat Med. 2016;2016:3915013. [PubMed: 27840652]

18. Csintalan RP, Inacio MCS, Funahashi TT, Maletis GB. Risk factors of subsequent operations after primary anterior cruciate ligament reconstruction. Am J Sports Med. 2014;42(3):619–625. [PubMed: 24335588]

19. Born CT, Gil JA, Goodman AD. Joint contractures resulting from prolonged immobilization: etiology, prevention, and management. Am Acad Orthop Surg. 2017;25(2):110–116.

20. Ohmichi Y, Sato J, Ohmichi M, et al. Two-week cast immobilization induced chronic widespread hyperalgesia in rats. Eur J Pain. 2012; 16(3):338–348. [PubMed: 22337282]

21. Derby B, Akhtar R. Mechanical properties of aging skeletal muscle. In: Derby B, Akhtar R, eds. Mechanical Properties of Aging Soft Tissues. Engineering Materials and Processes. Springer; 2015.

22. Wong K, Trudel G, Laneuville O. Noninflammatory joint contractures arising from immobility: animal models to future treatments. BioMed Res Int. 2015;2015:848290.

23. Schrumpf MA, Lyman S, Do H, et al. Incidence of postoperative elbow contracture release in New York State. J Hand Surg Am. 2013; 38(9):1746–1752. [PubMed: 23831364]

24. J Kojima S, Hoso M, Watanabe M, Matsuzaki T, Hibino I, Sasaki K. Experimental joint immobilization and remobilization in the rats. Phys Ther Sci. 2014;26(6):865–871.

25. Sasabe R, Sakamoto J, Goto K, et al. Effects of joint immobilization on changes in myofibroblasts and collagen in the rat knee contracture model. J Orthop Res. 2017;35(9):1998–2006. [PubMed: 27918117]

26. Ando A, Hagiwara Y, Onoda Y, et al. Distribution of type A and B synoviocytes in the adhesive and shortened synovial membrane during immobilization of the knee joint in rats. Tohoku J Exp Med. 2010;221(2):161–168. [PubMed: 20501969]
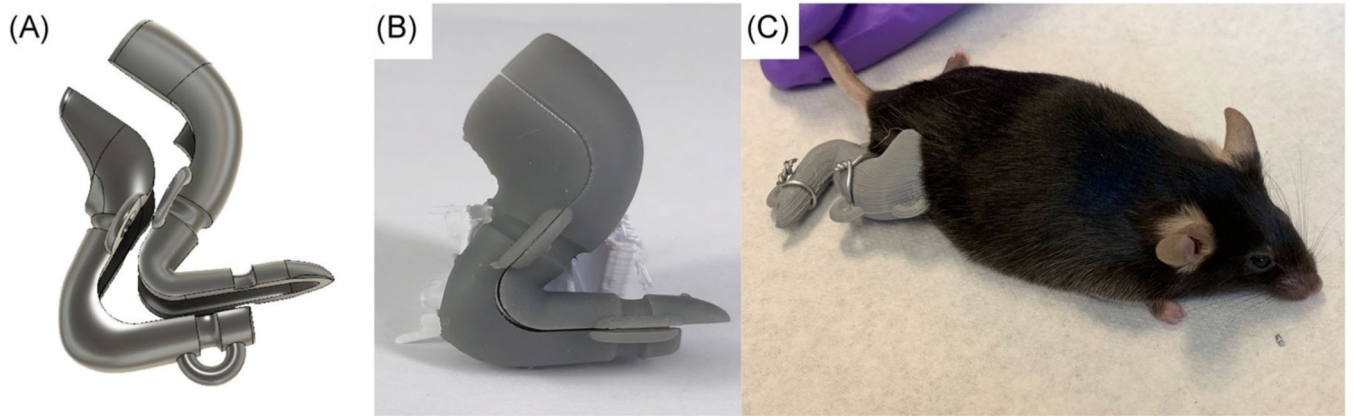
FIGURE 1.

Mouse clamshell cast design. (A) Clamshell cast design from AutoDesk Fusion 3D. (B) 3D printed clamshell cast in methacrylate resin. (C) Clamshell casts are secured to a single mouse hindlimb using 20G wire. 3D, three-dimensional
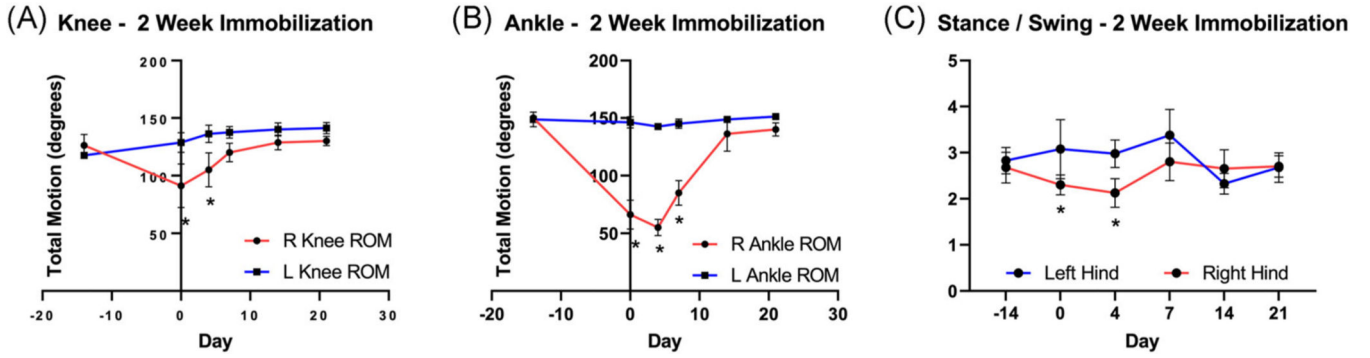
FIGURE 2.

Two-week immobilization of young mice. (A) Average mouse knee joint range of motion as measured by goniometer after 2 weeks of immobilization. Statistically significant difference in immobilized (right) versus control (left) limb on Days 0 and 4 (ANOVA, $p = 0.0002$, *$p < 0.001$, $n = 4$). (B) Average mouse ankle joint range of motion as measured by goniometer after 2 weeks of immobilization. Statistically significant difference on Days 0, 4, and 7 (ANOVA, $p < 0.0001$, *$p < 0.0001$, $n = 4$). (C) DigiGait® analysis of mouse gait, statistically significant difference in stance percentage in immobilized (right) versus control (left) limbs (ANOVA, $p = 0.01$ for time, *$p < 0.05$ right vs. left). ANOVA, analysis of variance
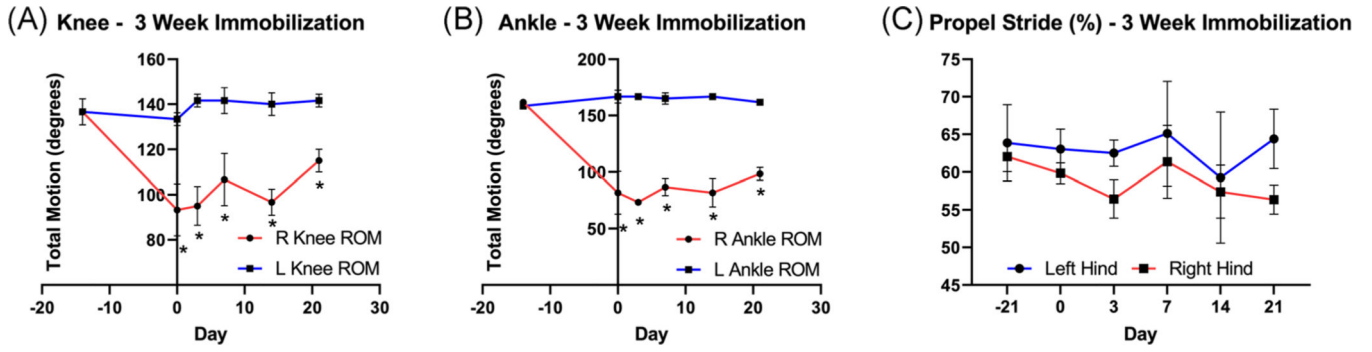
FIGURE 3.

Three-week immobilization of young mice. (A) Average mouse knee joint range of motion as measured by goniometer method after 3 weeks of immobilization. Statistically significant difference in immobilized (right) versus control (left) limb on Days 0, 4, 7, 14, and 21 (ANOVA, $p = 0.0013$, *$p < 0.001$ right vs. left, $n = 3$). (B) Average mouse ankle joint range of motion as measured by goniometer method after 3 weeks of immobilization. Statistically significant difference in immobilized (right) versus control (left) limb on Days 0, 4, 7, 14, and 21 (ANOVA, $p < 0.0001$, *$p < 0.0001$ right vs. left, $n = 3$). (C) DigiGait® analysis of mouse gait, propel stride percentage on right (immobilized) versus left (control) limbs (ANOVA, $p = 0.025$, $n = 3$)
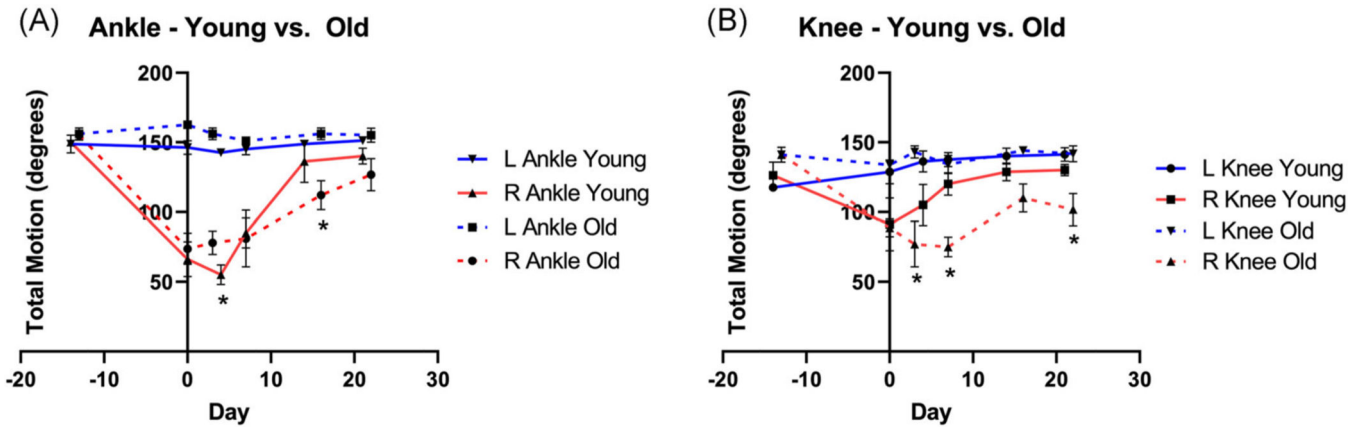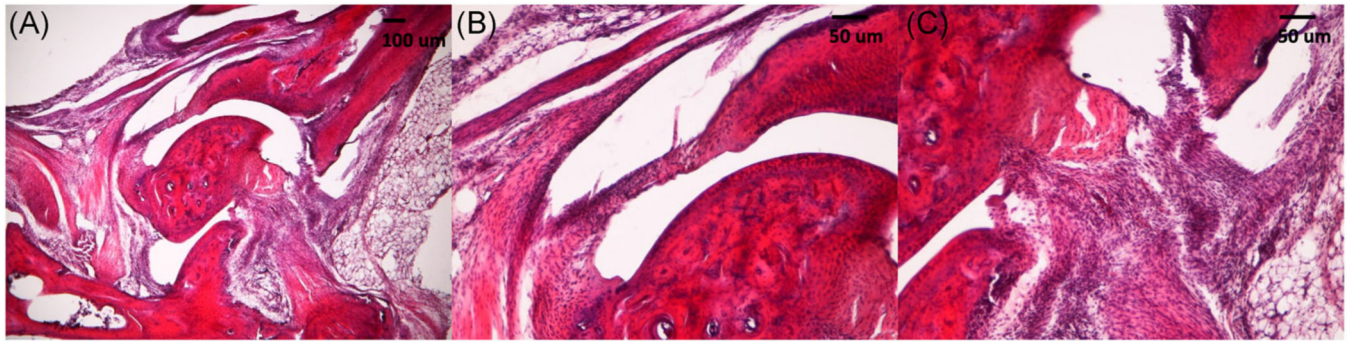
FIGURE 4.

Comparison of knee and ankle range of motion in old versus young mice. Average mouse joint range of motion as measured by goniometer after 2 weeks of immobilization of old and young mice. (A) Ankle range of motion significantly different on all days immobilized (right) versus control (left) limbs for old mice (mixed-effects model, $p < 0.0001$, $n = 5$). No significant difference in immobilized (right) ankle motion between old ($n = 5$) and young ($n = 4$) mice by mixed-effects model. Post hoc testing demonstrates difference in means at Day 4 ($p = 0.04$) and Day 14 ($p = 0.028$). (B) Knee range of motion significantly different for the immobilized (right) knee versus control (left) knees for old mice (mixed-effects model, $p < 0.0001$, $n = 5$). Significant difference in immobilized (right) knees between old ($n = 5$) and young ($n = 4$) mice by mixedeffects model ($p < 0.0001$). Post hoc testing significant on Day 3 ($p = 0.0045$), Day 7 ($p < 0.0001$), and Day 21 ($p = 0.013$)

FIGURE 5.
Representative hematoxylin and eosin staining of ankle sagittal sections from 8-month-old mice immobilized for 2 weeks. (A) Ankle joint at ×4. (B) Anterior ankle taken at ×20. (C) Posterior ankle was taken at ×20
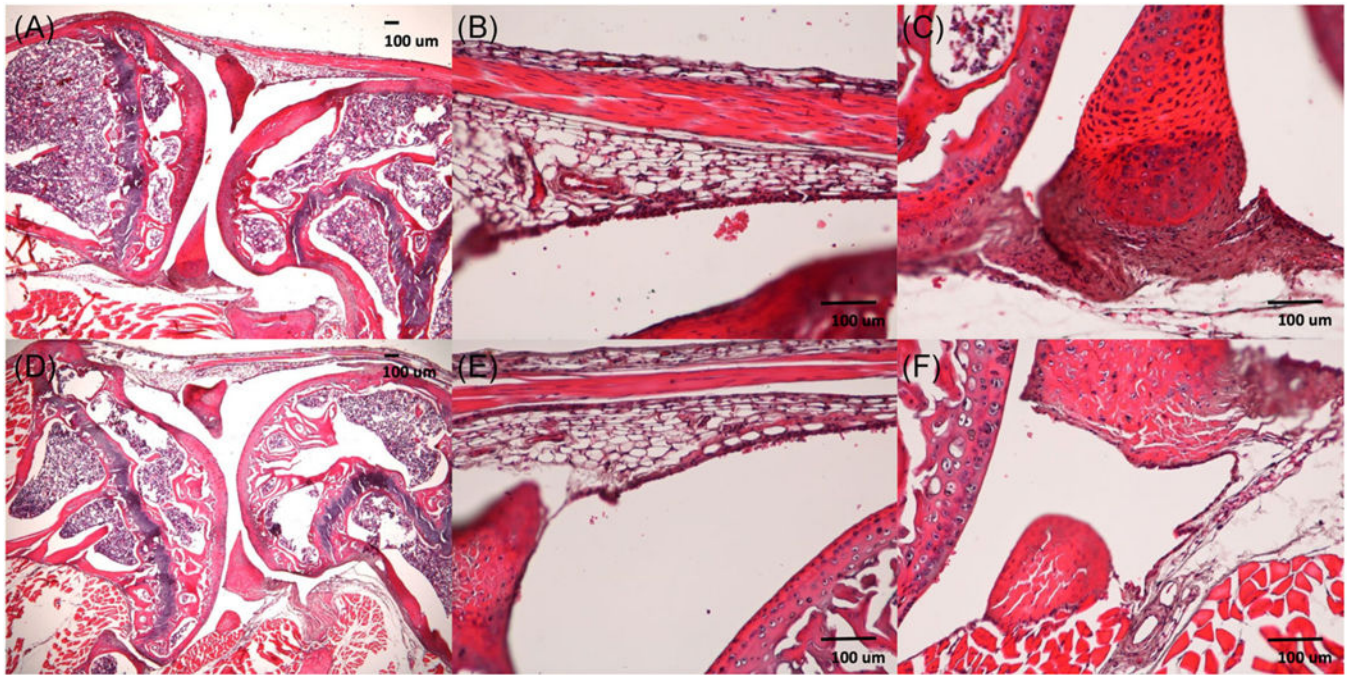
FIGURE 6.
Representative hematoxylin and eosin staining of knee sagittal sections from immobilized and control limbs of 8-month-old mice immobilized for 2 weeks. (A) Immobilized (right) knee taken at ×4. (B) Anterior fat pad of immobilized knee taken at ×20. (C) Posterior capsule and meniscus of immobilized knee taken at ×20. (D) Control (left) knee taken at ×4. (E) Anterior fat pad of control knee taken at ×20. (F) Posterior capsule and meniscus of control knee taken at ×20. Scale bars = 100 μm

TABLE 1

Flexion and extension loss and recovery of immobilized mouse hindlimb

	Knee flexion	Knee extension	Ankle dorsiflexion	Ankle plantarflexion
Two-week young				
Baseline	142 ± 5	−16 ± 4.8	150 ± 0	0 ± 0
Max loss	126 ± 16	−35 ± 4.1	128 ± 2.5	−68.7 ± 2.5
Max recovery	142 ± 2.9	−11 ± 6.3	147 ± 2.9	−6.25 ± 2.5
Three-week young				
Baseline	148.3 ± 2.9	−11.6 ± 2.9	162 ± 2.9	0 ± 0
Max loss	125 ± 8.6	−38 ± 2.9	126 ± 5.7	−60 ± 0
Max recovery	143 ± 2.9	−28.3 ± 2.9	141 ± 2.9	−30.0 ± 5.0
Two-week old				
Baseline	146 ± 5.4	−5 ± 0	155 ± 3.5	0 ± 0
Max loss	130 ± 4.1	−64 ± 11.4	123 ± 9.7	−60 ± 8.1
Max recovery	147 ± 6.7	−37 ± 8.4	148 ± 7.6	−21.6 ± 7.6